Bioinformatics Analysis and Experimental Verification of Prognostic and Biological Significance of Autophagy-Related Long Non-Coding RNAs in Gastric Carcinoma

Jiebang Jiang[1,2,3]*

[1]Center for Clinical Research and Translational Medicine, Yangpu Hospital, Tongji University School of Medicine, Shanghai 200090, China

[2]Institute of Gastrointestinal Surgery and Translational Medicine, Tongji University School of Medicine, Shanghai 200090, China

[3]Department of General Surgery, Yangpu Hospital Affiliated to Tongji University, Tongji University School of Medicine, Shanghai 200090, China

*****Corresponding author:** Jiebang Jiang, jjb_yzx@163.com

Abstract: *Background:* Long non-coding RNAs (lncRNAs) play a vital role in autophagy modulation and tumor progression. However, the key lncRNAs and their functions in gastric cancer (GC) remain largely unknown. *Methods:* A bioinformatic analysis of GC patients' gene expression profiling data from the Cancer Genome Atlas database was performed to identify autophagy-related lncRNAs that are associated with predictive risk. Through Cox regression and Lasso regression analyses, the autophagy-related lncRNAs that are associated with prognosis were identified, and a novel prognostic model for GC was established. The model was then used to evaluate the clinical features and predictive risk of individuals with GC. By using two datasets, GSE 62254 (n = 300) and GSE 15459 (n = 192), from Gene Expression Omnibus, its effectiveness was verified. Gene set enrichment analysis according to hallmark and Kyoto Encyclopedia of Genes and Genomes were used to determine the possible biological roles of these lncRNAs. Furthermore, the HOXD antisense growth-associated long non-coding RNA (HAGLR) mechanism in GC was discovered through *in vitro* and *in vivo* experiments. *Results:* Six lncRNAs associated with autophagy in GC were identified, and a new prognostic risk model based on these lncRNAs was established. The six-lncRNA signature was significantly associated with adverse clinicopathological features and found to be an independent GC prognostic factor. The model was proven to be effective and robust by GSE62254 and GSE15459. According to gene set enrichment analysis, the six lncRNAs appeared to be tightly linked to autophagy-related and cancer-related mechanisms. HAGLR was also found to promote tumor growth by enhancing autophagy signaling in GC. *Conclusion:* A novel prognostic model integrating HAGLR that can effectively evaluate and predict the prognostic risk of GC patients was established. The results indicated that HAGLR promotes gastric cancer progression by enhancing autophagy and is anticipated to be a potential new target for the treatment of gastric cancer.

Keywords: Gastric cancer; Autophagy; Long non-coding RNA; Prognostic risk; HAGLR

1. Introduction

Gastric cancer (GC) is one of the most life-threatening malignant tumors worldwide [1]. Although there has been tremendous progress in the management of this disease, the overall 5-year survival rate of individuals with GC is still low, as it is often diagnosed at an advanced stage [2]. Therefore, the treatment of GC is greatly challenged.

Long non-coding RNAs (lncRNAs) are RNAs with a length of 200 nucleotides or more with limited ability for protein-coding [3]. However, they tend to drive the formation and growth of malignant tumors by providing signals of malignant transformation through precise regulation of their own transcription [4]. Furthermore, lncRNAs dictate the autophagy role in tumors [5-7] and influence the degree of autophagy in various stages of cancer progression [8], thereby regulating tumor growth. Therefore, lncRNAs are known to be strictly associated with tumor progression [9-12]. In recent years, they have been widely utilized as prognostic and diagnostic markers of various cancers [13].

In this investigation, six autophagy-related lncRNAs associated with GC prognosis was identified to establish a novel prognostic model, which can facilitate early prognostic risk stratification and individualized treatment regimens for GC patients. The tumor-enhancing role of the lncRNAs and the HOXD antisense growth-associated long non-coding RNA (HAGLR) mechanism in GC were also explored and verified through experiments, thus presenting a new potential target for GC treatment.

2. Materials and methods

2.1. Flowchart of the study and data source

Supplementary Figure 1A shows the detailed workflow of the development and validation of the new predictive model of six autophagy-related lncRNAs in GC. The transcriptome and medical data of the training set, containing 375 gastric cancer specimens, were acquired from The Cancer Genome Atlas (TCGA) database. RNA-sequencing (RNA-Seq) information was downloaded in FPKM format and normalized to log2(FPKM+1). The corresponding clinical data of the patients included age, gender, overall TNM stage, individual TNM stage, tumor grade, overall survival (OS) status, and time. The gene expression profiles and medical data of 300 subjects with GC and 192 patients with GC obtained from Gene Expression Omnibus (GEO) datasets (GSE 62254 and GSE 15459) were used as verification data.

2.2. Autophagy-related long non-coding RNAs screening

Geno biotypes were annotated with genomic information from Homo sapiens (version GRCh38.99), and 14,081 and 1,105 lncRNAs were identified from TCGA and GEO datasets. Then, 222 and 328 genes related to autophagy were acquired from the Human Autophagy Database (HADb) and the Gene Ontology (GO) gene set (GOBP_REGULATION_OF_AUTOPHAGY, M10281) of Molecular Signatures Database (MSigDB), respectively. After removing duplicated genes, 495 genes related to autophagy were included for further analysis. By using $|R2| > 0.3$ and $P < 0.01$ as selection principles, Pearson correlation analysis between autophagy-related genes and lncRNAs was conducted to identify the lncRNAs related to autophagy in the TCGA dataset.

2.3. Competing endogenous (ce)RNA network construction

The miRcode database (http://www.mircode.org/) was used to predict microRNA (miRNA) and autophagy-related lncRNA relationship pairs. Three databases, TargetScan (http://www.targetscan.org/), miRTarBas (http://mirtarbase.cuhk.edu.cn/), and miRDB (http://mirdb.org/), were employed to obtain the experimentally validated interaction between these miRNAs and 495 autophagy-related messenger RNAs (mRNAs). Then, a ceRNA network was created using the lncRNAs, miRNAs, and mRNAs obtained by the above methods. Cytoscape 3.8.0 was used to visualize this network.

2.4. Prognostic risk model validation and construction

The overlapping genes from 1,105 lncRNAs obtained from the GEO datasets and cell autophagy-related lncRNAs identified in the TCGA dataset were employed for further analysis to establish a predictive risk model. First, univariate Cox regression analysis was performed to determine if the training group prognosis was substantially influenced by autophagy-related lncRNAs. Then, lncRNAs that overlapped with other lncRNAs were eliminated by Lasso regression analysis using the R package glmnet. Third, multivariate Cox regression analysis was performed to obtain a minimal gene set for prognostic risk prediction. The following formula was used to compute the prognostic risk score: risk score = coef1*expr1 + coef2*expr2 +…+ coefn*exprn. Coefn and exprn represent the coefficient and gene n expression value. The samples were distributed into low- and high-risk groups based on the median risk score as the critical value. Then, the difference in survival between low- and high-risk groups was assessed using Kaplan-Meier survival analysis.

In order to further analyze the relationship between the risk score and clinicopathological factors, age, sex, overall TNM stage, individual TNM stage, tumor grade, and risk score were all included in the multivariate and univariate Cox regression analyses to determine if risk score is an independent prognostic factor in individuals with GC. A multi-indicator receiver operating characteristic (ROC) curve was employed to evaluate the risk scoring precision in the prognosis of individuals with GC. The assessment of this risk scoring model's stability was performed in a similar manner using the GEO datasets as a validation dataset.

2.5. Gene set enrichment analysis

The functional difference between the low- and high-risk groups was estimated by gene set enrichment analysis. In this study, GSEA was employed to identify the potential function enriched in the high-risk group that most likely leads to a poor prognosis.

2.6. Cell culture and transfection

Normal gastric epithelial cell line GES-1 and GC cell lines AGS and SGC-7901 were obtained from the Cell Bank of the Chinese Science Academy. The cells were kept in Roswell Park Memorial Institute (RPMI) 1640 medium (Thermo Fisher Scientific, Inc.) supplemented with 1% penicillin-streptomycin (Sigma-Aldrich) and 10% fetal bovine serum (FBS; Gibco) at 37°C under 5% carbon dioxide (CO_2). Negative control small interfering RNA (si-NC), small interfering RNA against HAGLR (si-HAGLR)#1, and si-HAGLR#2 were designed and created in GenePharma Inc. and transfected into cells following the manufacturer's protocol. **Supplementary Table S1** shows the si-NC, si-HAGLR#1, and si-HAGLR#2 sequences.

2.7. RNA extraction and quantitative real-time polymerase chain reaction

TRIzol reagent was used to extract the total RNA from cells and tissues (Thermo Fisher, USA). PrimeScript™ reverse transcription (RT) kit (Takara, Kyoto, Japan) was used to transcribe complementary DNA reversibly, and TB Green Premix Ex Taq™ II kit (Takara, Kyoto, Japan) was employed to determine the expression quantity through quantitative real-time PCR (qPCR) following the manufacturer's protocol. β-actin was utilized as an internal reference. **Supplementary Table S1** shows the primer sequences utilized for qPCR by means of $2^{-\Delta\Delta CT}$ to analyze relative gene expression.

2.8. Cell proliferation assay

AGS cells (10^3 cells/well) were plated into 96-well plates. The well was injected with 10 μL Cell Counting Kit-8 (CCK-8) assay (Beyotime) and incubated for 4 h at 37°C. The absorbance was detected at 450 nm to

determine cell growth. For the colony formation assay, 2×10^3 AGS cells were supplemented to six-well plates. The cells were incubated the following day in conditioned media, which was changed every three days. Cell colonies were fixed with 4% polyformaldehyde and stained with 0.1% crystal violet on the tenth day. The quantity of cell colonies was then calculated.

2.9. Transwell assay
A cell migration test was performed on 24-well transwell cell culture chambers with 8-μm diameter holes (Corning, USA); 200 μL serum-free medium suspension containing 2×10^5 AGS cells was introduced to the superior chambers, while 750 μL complete culture medium was injected into the inferior chambers. After one day, the remaining superior chamber cells were eliminated, and the inferior chamber cells were stained with 0.1% crystal violet and fixed with 4% paraformaldehyde. The cells were counted after at least five randomized microscopic fields were captured on camera (at 100× magnification).

2.10. Western blot
Western blot was performed as described in previous research [14]. Secondary antibodies (1:2000; Jackson ImmunoResearch), β-actin (1:10000; Abcam), and primary antibodies against microtubule-associated protein 1A/1B-light chain 3 (LC3B, 1:1000; Proteintech) were used.

2.11. Immunofluorescence assay
The inoculated cells were seeded onto a glass coverslip in a 24-well plate. After that, the cells were permeabilized for 15 min with 0.5% Triton X-100 at room temperature and then fixed for 30 min with 4% paraformaldehyde. Primary anti-LC3B antibodies (1:300; Invitrogen) were incubated on cells before adding Goat Anti-Rabbit Alexa Fluor 488 (1:400; Jackson ImmunoResearch). The BX53 Fluorescence Microscope (Olympus) was used to capture images, while the nuclei were stained with 4',6-diamidino-2-phenylindole (DAPI).

2.12. Mice tumor models
The Institutional Animal Care and Use Committee of Tongji University (LL-2021-SCI-005) authorized all animal investigations conducted following the National Institutes of Health (NIH) Strategies for the Care and Use of Laboratory Animals. Thirty female nude mice (BALB/c, 6weeks, 18–20 g) were obtained from Shanghai Jiesijie Lab Animals Co., Ltd. for two experiments. In the first experiment, 15 mice were assigned to two groups (7 mice in the si-NC group and 8 mice in the si-HAGLR group). The cell suspension (1×10^7 cells/100 μL) was injected subcutaneously in the mid-dorsal region of the mice. All mice were observed, and the observations were recorded once every 3 days. The following formula was used to estimate the cancer volume: volume = (length × width^2)/2. The nude mice were killed after 21 days, and the cancers were photographed and quantified. Western blot analysis was performed to determine if LC3B was expressed in the malignant tissues of nude mice. The experiment was repeated using the same number of mice in each group as that in the first experiment.

2.13. Statistical analysis
Data analysis was performed, and plots were generated using R program version 4.0.0. One-way analysis of variance (ANOVA) was carried out for multiple comparisons, while Student's t-test was employed for two-group comparisons. Data were expressed in mean ± standard error of mean (SEM). A *P*-value smaller than 0.05 was identified to be statistically significant.

3. Results

3.1. Autophagy-related competing endogenous RNA network

After performing Pearson correlation analysis between lncRNAs and autophagy-related genes in the TCGA dataset, 843 lncRNAs were recognized as autophagy-related lncRNAs using $|R^2| > 0.3$ and $P < 0.01$ as the threshold. Thirty-four autophagy-related lncRNA and miRNA relationship pairs were obtained through miRcode. Then, TargetScan, miRTarBas, and miRDB were utilized to predict the relationship between autophagy-related genes and miRNA. An autophagy-related ceRNA network was obtained, which included 33 lncRNAs, 29 miRNAs, and 75 mRNAs (**Supplementary Figure 1B**).

3.2. Building a predictive risk model based on autophagy-related lncRNAs

A total of 136 autophagy-related lncRNAs were filtered after the overlap between the 843 autophagy-related lncRNAs in the TCGA dataset and the 1,105 GEO lncRNAs. Based on the TCGA dataset, 136 autophagy-related lncRNAs were associated with the survival data of GC patients, and 10 autophagy-related lncRNAs were found to be associated with prognosis by univariate Cox regression analysis (**Figure 1A**). Two autophagy-related lncRNAs were eliminated by Lasso Cox regression analysis (**Figure 1B–C**). Multivariate Cox regression analysis showed that six lncRNAs with prognostic significance, namely LINC01023, LINC00963, HAGLR, MIR100HG, LINC01315, and LINC00857, were associated with autophagy (**Figure 1D**). The following formula was used to estimate the risk score for individuals with GC: risk score = $(0.379944 \times$ LINC01023$) + (-0.32266 \times$ LINC00963$) + (0.316604 \times$ HAGLR$) + (0.158644 \times$ MIR100HG$) + (-0.56624 \times$ LINC01315$) + (-0.19173 \times$ LINC00857$)$. GC patients were distinguished as high-risk (n = 175) and low-risk (n = 175) groups based on the median risk score. Kaplan-Meier survival curve revealed that GC patients with elevated risk score showed significantly shorter OS (median OS: 383 days versus 526 days; $P < 0.001$; **Figure 1E**). GC patients were ranked based on their risk scores (**Figure 1F**), and the scatter dot plot (**Figure 1G**) showed that patients with higher risk scores had shorter survival. The heatmap showed significant difference in lncRNA levels related to 6 prognostic signals between low- and high-risk individuals with GC (**Figure 1H**). Furthermore, there were significant group differences in the expression of all six autophagy-related lncRNAs (**Supplementary Figure 1C–H**; high- versus low-risk scores; $P < 0.05$).

3.3. Correlation between autophagy-related long non-coding RNA predictive risk score and clinicopathological factors

From the association between autophagy-related lncRNA predictive risk score and age, gender, tumor grade, overall TNM stage, and individual TNM stage, the outcomes indicated that there was no significant difference in the risk scores between age > 60 and ≤ 60 as well as between men and women (**Supplementary Figure 1I–J**). However, the risk score was higher in stage II–IV than in stage I ($P < 0.05$) and in G3 than in G1–2 ($P < 0.001$; **Supplementary Figure 1K–L**). These outcomes indicate that risk score may be associated with GC progression.
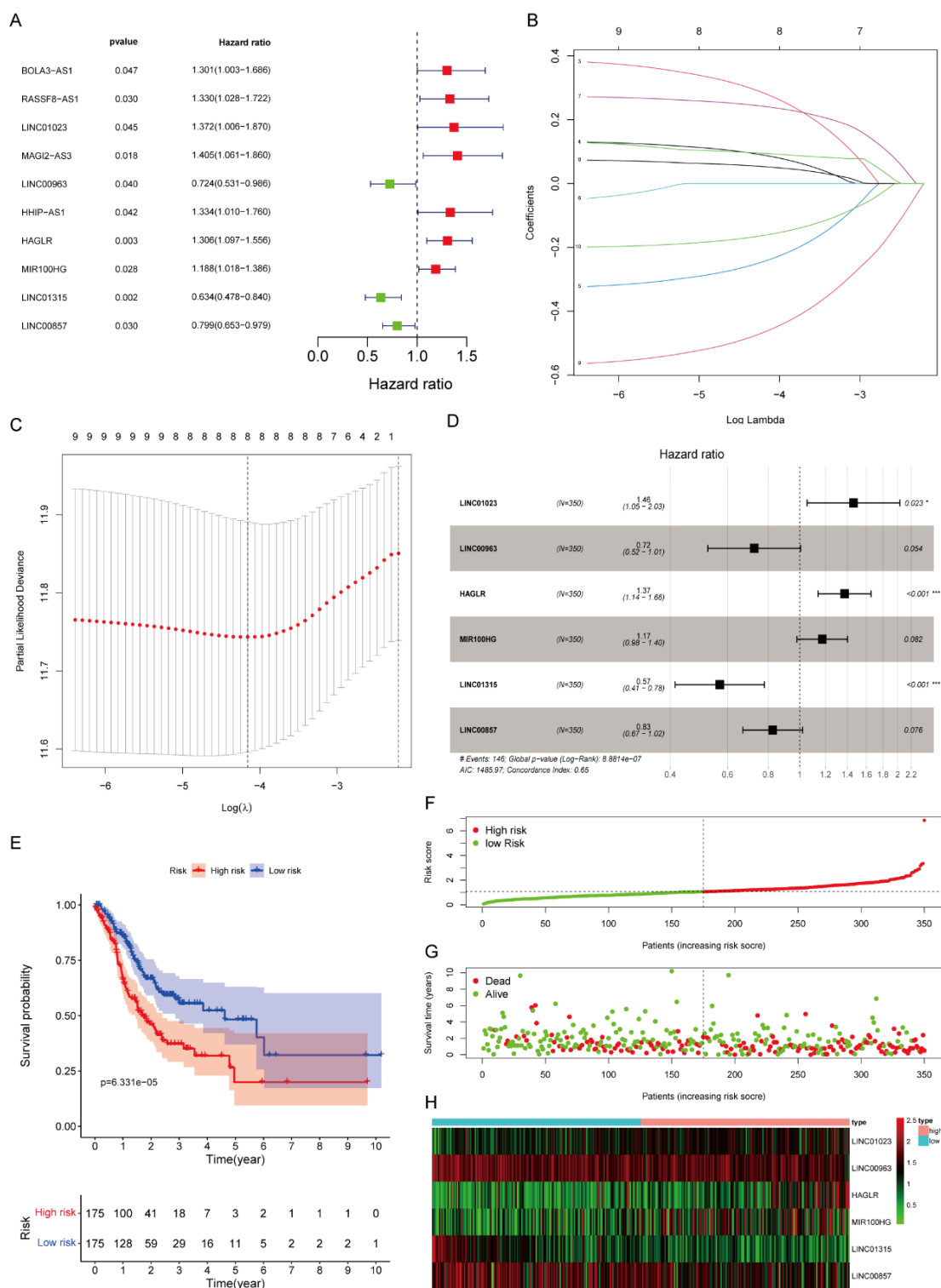
Figure 1. (A) Forest plot of hazard ratios showing 10 autophagy-related long non-coding (lnc)RNAs associated with overall survival in gastric cancer (GC). (B) Lasso coefficient profiles of prognostic lncRNAs. (C) Lasso coefficient values and vertical dashed lines at the best log (lambda) value. (D) Six prognostic autophagy-related lncRNAs in GC. (E) Kaplan-Meier survival analysis of high- and low-risk groups based on the risk model for GC patients in The Cancer Genome Atlas database. (F) Distribution of risk scores for each patient. (G) Survival status of GC patients. (H) Expression heatmap of six autophagy-related lncRNAs.

3.4. The six-autophagy-related lncRNAs risk score is an independent prognostic factor in GC

Univariate Cox regression analysis was performed to prove that the six incRNAs are independent prognostic factors. The analysis showed that many factors, including age and sex, were associated with OS (**Figure 2A**). Multivariate analysis showed that autophagy-related lncRNA predictive risk score and age were significantly linked to OS (**Figure 2B**). According to the ROC curve, the area under the curve (AUC) of the autophagy-related lncRNA prognostic risk score was 0.705 (**Figure 2C**). On the basis of these findings, the autophagy-related lncRNA predictive risk score is an independent prognostic factor for individuals with GC.
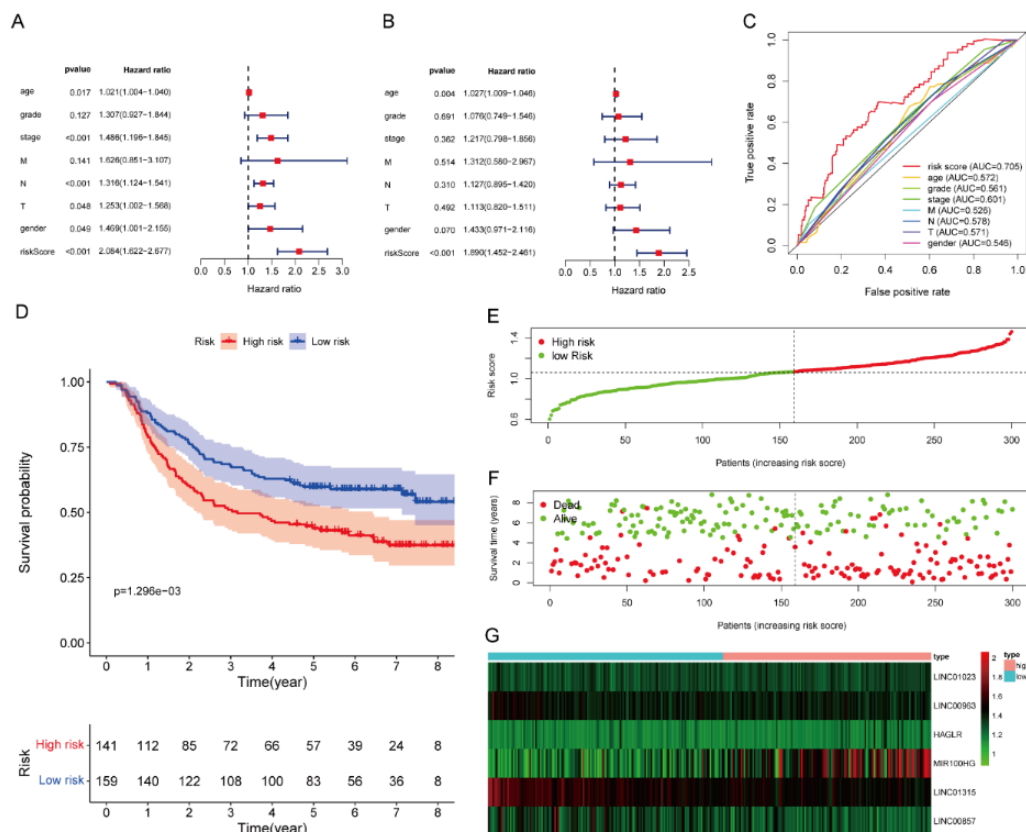
Figure 2. (A) Univariate Cox regression analysis for risk score, age, gender, tumor grade, overall TNM stage, and individual TNM stage. (B) Forest plot for multivariate Cox regression analysis showing that risk score and age were independent prognostic factors. (C) Multivariate receiver operating characteristic curve analysis showed predictive accuracy of the prognostic signature. (D) Kaplan-Meier survival analysis of high- and low-risk groups based on the risk model for gastric cancer (GC) patients in the Gene Expression Omnibus dataset (GSE62254). (E) Distribution of risk scores for each patient. (F) Survival status of GC patients. (G) Expression heatmap of six autophagy-related long non-coding RNAs.

3.5. Prognostic risk model validation in the Gene Expression Omnibus datasets

Two independent validation datasets (GSE62254 and GSE15459) from the GEO database were employed to evaluate the validity of the prognostic risk model. First, the risk score for GC patients was estimated depending on the six lncRNAs expression in the GEO datasets. The patients in the two GEO cohorts were distributed into high- and low-risk groups based on the TCGA cohort median risk score. According to Kaplan-Meier survival curve analysis, GC patients with high-risk scores had significantly shorter OS than those with low-risk scores (**Figure 2D** and **Supplementary Figure 2A**). The survival status, risk score, and lncRNAs expression pattern distributions of the high- and low-risk groups in the validation sets are shown in **Figure 2E–G** and **Supplementary Figure 2B–D**. These outcomes showed consistent trends in those

observed in the TCGA dataset. Furthermore, the ROC curve indicated that the AUC values of the autophagy-related lncRNA prognostic risk model were 0.615 and 0.598 (**Supplementary Figure 2E**–**F**). Overall, the above outcomes indicate that this established prognostic risk model of six autophagy-related lncRNAs can provide reliable prognostic risk prediction for GC patients.

3.6. Gene set enrichment analysis

GSEA was performed for both low- and high-risk groups of the lncRNA prognostic risk model. The analysis showed that 40 mechanisms were significantly enriched in the high-risk group (**Supplementary Table 2**). These mechanisms include many important tumor-related signaling pathways, such as interleukin
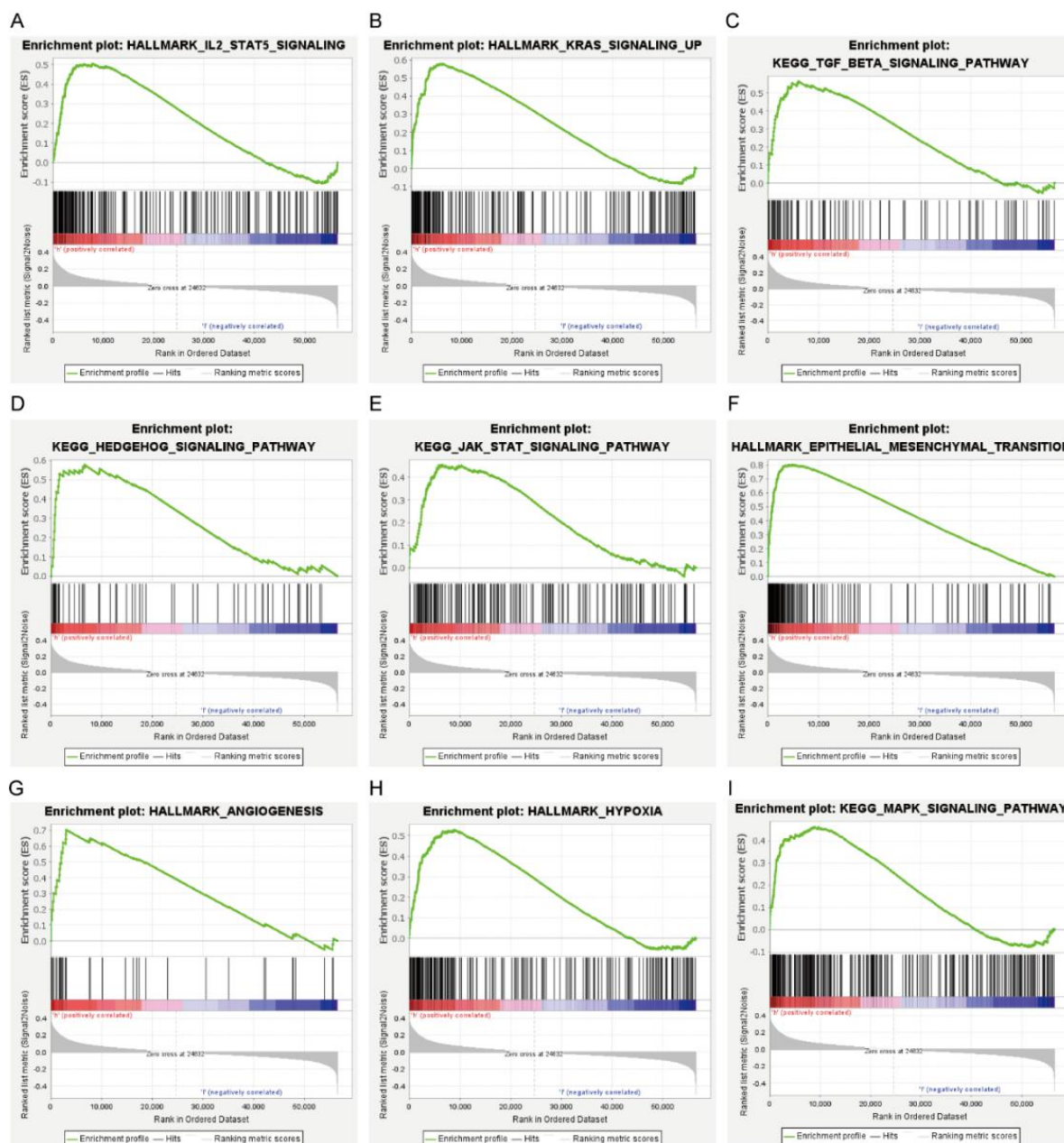
Figure 3. (A–E) Gene set enrichment analysis indicated significant enrichment of multiple cancer-related pathways in the high-risk group based on The Cancer Genome Atlas database. (F–G) Two major pathways associated with tumor progression and metastasis were significantly enriched in the high-risk group. (H–I) Autophagy signaling pathways that were significantly enriched in the high-risk group (determined by gene set enrichment analysis).

2 (IL2)/signal transducer and activator of transcription 5 (STAT5), Kirsten rat sarcoma viral oncogene homolog (KRAS), transforming growth factor beta (TGF-β), Hedgehog, and Janus kinase (JAK)/STAT signaling pathways (**Figure 3A–E**), as well as epithelial-mesenchymal transition and angiogenesis pathways, both of which are involved in cancer invasion and metastasis (**Figure 3F–G**). Moreover, hypoxia and mitogen-activated protein kinase (MAPK) signaling pathways that are closely associated with autophagy were observed in the high-risk group (**Figure 3H–I**). The above outcomes indicate that these autophagy-related lncRNAs are closely associated with tumor formation and progression.

3.7. HAGLR promotes gastric cancer cell proliferation and migration
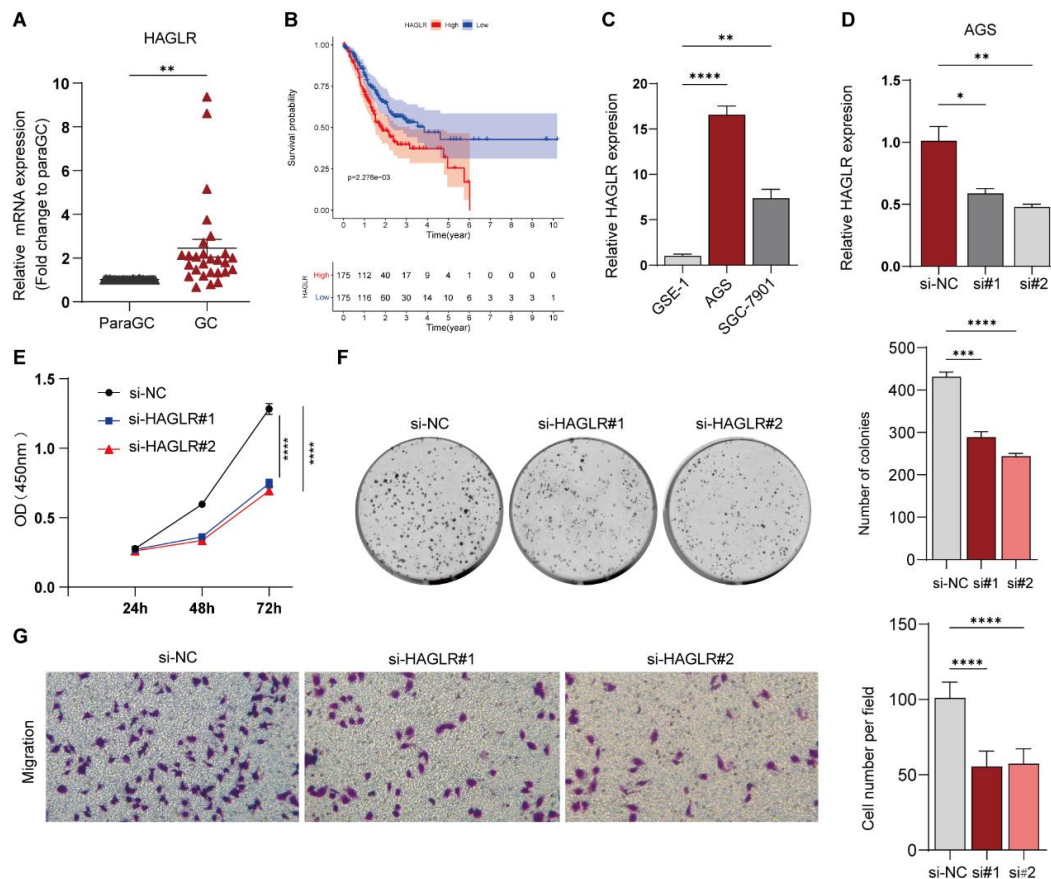
Figure 4. (A) qPCR analysis of HAGLR messenger RNA expression levels in human paired GC tissues and adjacent tissues. (B) Kaplan-Meier survival analysis of GC patients from TCGA database showing HAGLR as a significant prognostic risk factor for patients with GC ($P < 0.01$). (C) The expression levels of HAGLR in GSE-1, AGS, and SGC-7901 were assessed by qPCR. (D) The efficiency of MSR1 knockdown was confirmed by qPCR. (E–F) The proliferation ability of AGS cells after HAGLR knockdown was measured by (E) CCK-8 and (F) colony formation assays. (G) The effect of HAGLR knockdown on AGS cells migration was measured by transwell migration. Representative images showing the results of the assays. Magnification: 100× (left panel). Histogram showing the number of migration cells (right panel). Data are displayed as mean ± SEM; *$P < 0.05$, **$P < 0.01$, ***$P < 0.001$, and ****$P < 0.0001$; Paired Student's t-test (A) for two-group comparisons, and one-way ANOVA (C–D and F–G) or two-way ANOVA (E) with Tukey's method for multiple comparisons. Abbreviations: ANOVA, analysis of variance; CCK-8, Cell Counting Kit-8; GC, gastric cancer; HAGLR, HOXD antisense growth-associated long non-coding RNA; qPCR, quantitative polymerase chain reaction; SEM, standard error of mean; si-NC, negative control small interfering RNA; si-HAGLR, small interfering RNA against HAGLR; TCGA, The Cancer Genome Atlas.

From the six lncRNAs identified, the HAGLR with the largest AUC value was selected for further research (**Supplementary Figure 2G**). The qPCR results of 27 pairs of GC and nearby healthy tissues revealed significantly increased HAGLR expression in GC tissues (**Figure 4A**); furthermore, patients with increased HAGLR expression had shorter survival time (**Figure 4B**), suggesting that HAGLR, as an oncogene, may be involved in GC development and thus affect the prognosis of patients. In addition, the elevated HAGLR expression in AGS cells was found to be significantly more than that in GSE-1 cells by qPCR detection (**Figure 4C**). In AGS cells, HAGLR expression was suppressed by siRNA HAGLR transfection (**Figure 4D**). Then, CCK-8 and colony formation assays were used to identify HAGLR impact on GC cells' growth ability; it was found that HAGLR knockout effectively inhibited AGS cells' growth ability (**Figure 4E–F**). Besides, AGS cells' migratory capability was also impaired following HAGLR knockdown, as shown in **Figure 4G**. These results suggest that HAGLR contributes to tumor proliferation and migration.

3.8. HAGLR promotes gastric cancer cell growth by enhancing autophagy *in vitro*
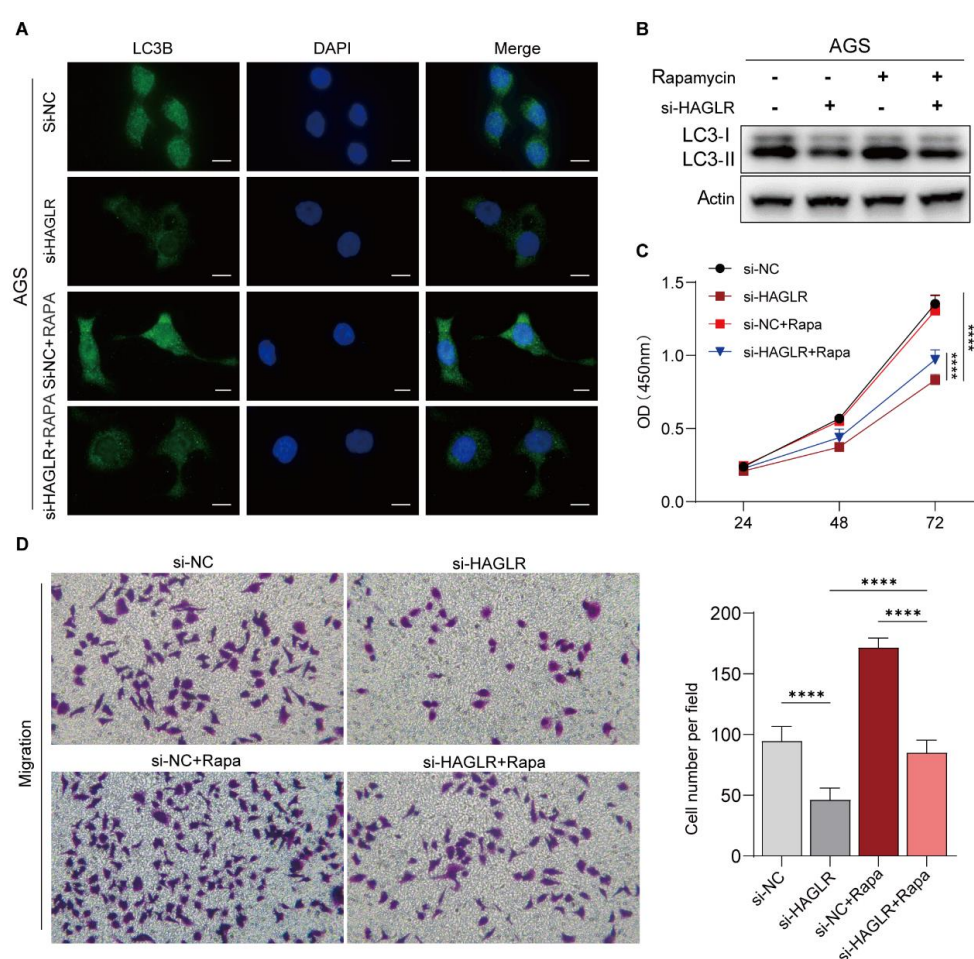
Figure 5. (A) HAGLR-knockdown AGS cells were treated with 1 μM rapamycin over 6 h for the rescue assay, and autophagy-related protein LC3B expression was detected by immunofluorescence staining (scale bar: 10 μm). (B) Western blot analysis of LC3B expression in rescue assay. (C) The proliferative capacity of AGS cells in the rescue assay was detected by CCK-8. (D) Cell migration was evaluated in the rescue assay by transwell migration assay. Magnification: 100× (left panel). Histogram showing the number of migration cells (right panel). Abbreviations: CCK-8, Cell Counting Kit-8; DAPI, 4',6-diamidino-2-phenylindole; HAGLR, HOXD antisense growth-associated long non-coding RNA; RAPA/Rapa, rapamycin; si-NC, negative control small interfering RNA; si-HAGLR, small interfering RNA against HAGLR.

In order to further investigate the potential influence of HAGLR regulatory pathway on GC progression, immunofluorescence staining and western blot were performed. It was discovered that when HAGLR was knocked out, the aggregation of LC3B protein in AGS cells was significantly suppressed (**Figure 5B**) and LC3B protein expression was significantly reduced, indicating an inhibition of autophagy flux. However, the inhibition of LC3B protein aggregation and expression caused by HAGLR silencing was rescued when AGS cells were treated with rapamycin to increase their autophagic flux (**Figure 5A**–**B**). Interestingly, rapamycin also compensated for the diminished cell proliferation (**Figure 5C**) and migration (**Figure 5D**) ability caused by HAGLR silencing. Overall, HAGLR can promote the growth of GC cells by enhancing autophagy.

3.9. HAGLR promotes gastric cancer progression by enhancing autophagy *in vivo*
In order to verify the above findings, a mice tumor model was established by subcutaneous introduction of AGS cells. It was found that HAGLR silencing significantly inhibited local tumor formation (**Figure 6B**); the subcutaneous cancers in the HAGLR knockdown group were smaller and lighter (**Figures 6A** and **6C**). Furthermore, the silencing of HAGLR suppressed LC3B expression in tumor tissues (**Figure 6D**). These outcomes indicate that HAGLR may be an important regulator of autophagy signaling that promotes GC development and a potential target in GC treatment.
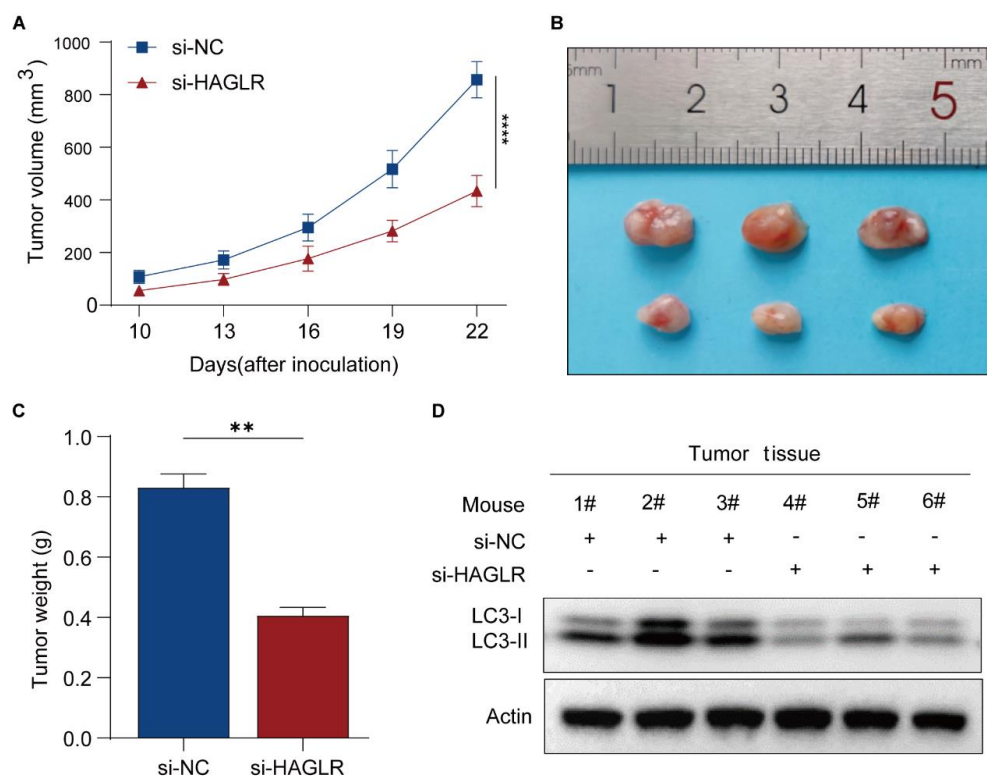
Figure 6. (A) Subcutaneous tumor volumes in the si-NC and si-HAGLR groups determined at the indicated time points. N = 6–8 animals per group. (B) Representative image of subcutaneous tumors at day 22. (C) Weight of the isolated tumor tissues. (D) Western blot analysis of the expression of autophagy-related protein LC3B in tumor tissues of the two groups of mice. Abbreviations: HAGLR, HOXD antisense growth-associated long non-coding RNA; si-NC, negative control small interfering RNA; si-HAGLR, small interfering RNA against HAGLR.

4. Discussion
Investigations have revealed that lncRNAs are related to autophagy modulation in tumors and can regulate autophagy via various mechanisms [8,15]. The most typical example is the equivalence of lncRNAs to

molecular sponges in modulating the expression of autophagy-related genes by absorbing autophagy-related miRNAs [9-11, 16]. Moreover, most autophagy-related lncRNAs influence tumor formation and progression [12]. Therefore, autophagy-related lncRNAs are very promising targets for cancer treatment and prognostic evaluation. In recent years, investigations on the predictive value of autophagy-related lncRNAs in different malignancies have been carried out.

Jiang *et al.* have built a predictive model of 16 autophagy-related lncRNAs, which can accurately predict the prognosis of lung cancer patients [13]. A study has identified six autophagy-related lncRNAs to build a model of risk score, which has been proven to be effective in differentiating between high and low-risk colorectal tumor patients as well as in predicting their OS [17]. In endometrial cancer, a predictive signature of five autophagy-related lncRNAs has also been developed. Compared with other traditional clinical indicators, this signature has been proven to be more efficient as an independent prognostic factor for endometrial cancer [18]. Although advances have been made in this field, the prognostic significance of autophagy-related lncRNAs in GC has yet to be investigated.

In the present study, autophagy-related genes were obtained from HADb and MSigDB, while the RNA sequence and medical data of GC patients were acquired from the TCGA database. Pearson correlation analysis was used to evaluate the association between autophagy-related genes and lncRNAs to identify autophagy-related lncRNAs. An autophagy-related ceRNA network was established based on these autophagy-related lncRNAs using four databases (miRcode, miRDB, miRTarBas, and TargetScan). Thereafter, univariate, multivariate, and lasso Cox analyses were performed to screen six autophagy-related lncRNAs (LINC01023, LINC00963, HAGLR, MIR100HG, LINC01315, and LINC00857), and a novel model of risk score that can precisely predict OS in individuals with GC was thus established. According to the model, the OS of GC patients in the high-risk group was significantly shorter. Moreover, in comparison to traditional medical prognostic factors, this risk scoring model has better predictive performance and can be assumed as an independent predictive factor for GC prognosis. This study validated this model to be effective and robust in predicting GC prognosis through two independent GEO datasets.

Among the six autophagy-related lncRNAs in the risk scoring model, LINC00857, MIR100HG, and LINC00963 have been established to be upregulated in GC patients with the worse prognosis; they have also been established as independent prognostic biomarkers of GC [19-21]. The other three lncRNAs (LINC01023, LINC01315, and HAGLR) are novel lncRNAs that have been identified in GC. Yu *et al.* have found that LINC01023 has an oncogenic function in glioma through IGF1R/AKT pathway activation and can be an applicable treatment target [22]. LINC01315, on the other hand, can facilitate the development and invasion of papillary thyroid carcinoma cells and colorectal cancer cells by sponging miR-497-5p and miR-205-3p, respectively [23, 24]. According to reports, HAGLR, which promotes colon tumor growth through the miR-185-5p/CDK4/CDK6 axis, is a potential target for colon cancer [25]. These studies demonstrate that these lncRNAs are very important in cancer progression; however, the biological processes involved remain unclear. In order to determine the underlying pathway of these lncRNAs in cancers, GSEA analysis was performed in the present study; it was found that mechanisms related to malignancy and autophagy were substantially enriched in the high-risk group. Interestingly, most of the cancer-related pathways enriched are closely associated with autophagy. For example, TGF-β signaling can regulate autophagy [26], and oncogenic KRAS can prompt NIX-mediated mitophagy to promote pancreatic malignancy [14]. The six autophagy-related lncRNAs identified in the present study are closely associated with GC formation and progression; they might influence GC progression by regulating autophagy, thus providing a reliable basis for future molecular mechanism research. A growing body of evidence has demonstrated that HAGLR possesses tumor-promoting ability; for instance, LncRNA-HAGLR can promote the development of triple-negative breast cancer via Wingless-type MMTV integration site family, member 2 (WNT2) regulation by sponging miR-335-3p [27] and colon cancer by sponging miR-185-5p and

triggering CDK4 and CDK6 [25]. The present study showed that individuals with GC and high HAGLR expression had shorter survival time, thus suggesting that HAGLR may have the ability to promote malignant GC development. Nevertheless, to date, whether HAGLR can regulate autophagy in CG and influence its malignant progression remains unclear. In the present study, *in vitro* experiments demonstrated that HAGLR promoted tumor cell growth and migration by enhancing autophagic flux in GC cells, while *in vivo* experiments demonstrated that HAGLR regulated autophagy-related pathways and promoted subcutaneous tumor growth in mice, thus further validating the *in vitro* results. These findings suggest that HAGLR can promote GC progression by enhancing autophagy.

5. Conclusion

A novel predictive signature integrating HAGLR was established in the present study. This predictive signature may contribute to individualized treatment and the follow-up of patients with GC. *In vitro* and *in vivo* experiments confirmed that HAGLR can promote GC progression by enhancing autophagy, thus suggesting this lncRNA as a potential novel target in GC treatment.

Funding

Disclosure statement

The author confirms that there were no financial or commercial relations that could be considered as having possible conflict of interest.

Author Contributions

This is a single-authored paper. The author confirms sole responsibility for the following: conceptualization, data curation, methodology, writing of original draft and revision, as well as visualization, including figure preparation.

Availability of data

In this investigation, publicly accessible datasets were examined. This information is available here: https://portal.gdc.cancer.gov/ and https://www.ncbi.nlm.nih.gov/gds/.

References

[1] Sung H, Ferlay J, Siegel RL, et al., 2021, Global Cancer Statistics 2020: GLOBOCAN Estimates of Incidence and Mortality Worldwide for 36 Cancers In 185 Countries. CA Cancer J Clin, 71(3): 209–249.

[2] Sexton RE, Al Hallak MN, Diab M, et al., 2020, Gastric Cancer: A Comprehensive Review of Current and Future Treatment Strategies. Cancer Metastasis Rev, 39(4): 1179–1203.

[3] Iyer MK, Niknafs YS, Malik R, et al., 2015, The Landscape of Long Noncoding RNAs in the Human Transcriptome. Nat Genet, 47(3): 199–208.

[4] Schmitt AM, Chang HY, 2016, Long Noncoding RNAs in Cancer Pathways. Cancer Cell, 29(4): 452–463.

[5] Janku F, McConkey DJ, Hong DS, et al., 2011, Autophagy as a Target for Anticancer Therapy. Nat Rev Clin Oncol, 8(9): 528–539.

[6] Xu J-L, Yuan L, Tang Y-C, et al., 2020, The Role of Autophagy in Gastric Cancer Chemoresistance: Friend or Foe?. Front Cell Dev Biol, 8: 621428.

[7] Islam Khan MZ, Tam SY, Law HKW, 2018, Autophagy-Modulating Long Non-Coding RNAs (LncRNAs) and Their Molecular Events in Cancer. Front Genet, 9: 750.

[8] Barangi S, Hayes AW, Reiter R, et al., 2019, The Therapeutic Role of Long Non-Coding RNAs in Human Diseases: A Focus on the Recent Insights into Autophagy. Pharmacol Res, 142: 22–29.

[9] Li C, Zhao W, Pan X, et al., 2020, LncRNA KTN1-AS1 Promotes the Progression of Non-Small Cell Lung Cancer Via Sponging of Mir-130a-5p and Activation of PDPK1. Oncogene, 39(39): 6157–6171.

[10] Lu M, Qin X, Zhou Y, et al., 2020, LncRNA HOTAIR Suppresses Cell Apoptosis, Autophagy and Induces Cell Proliferation in Cholangiocarcinoma by Modulating the miR-204-5p/HMGB1 Axis. Biomed Pharmacother, 130: 110566.

[11] Wang B, Xu L, Zhang J, et al., 2020, LncRNA NORAD Accelerates the Progression and Doxorubicin Resistance of Neuroblastoma Through Up-Regulating HDAC8 Via Sponging miR-144-3p. Biomed Pharmacother, 129: 110268.

[12] Yang L, Wang H, Shen Q, et al., 2017, Long Non-Coding RNAs Involved in Autophagy Regulation. Cell Death Dis, 8(10): e3073.

[13] Jiang A, Liu N, Bai S, et al., 2021, Identification and Validation of an Autophagy-Related Long Non-Coding RNA Signature as a Prognostic Biomarker for Patients with Lung Adenocarcinoma. J Thorac Dis, 13(2): 720–734.

[14] Humpton TJ, Alagesan B, DeNicola GM, et al., 2019, Oncogenic KRAS Induces NIX-Mediated Mitophagy to Promote Pancreatic Cancer. Cancer Discov, 9(9): 1268–1287.

[15] Ghafouri-Fard S, Shoorei H, Mohaqiq M, et al., 2021, Exploring the Role of Non-Coding RNAs in Autophagy. Autophagy, 2021: 1–22.

[16] Huang F, Chen W, Peng J, et al., 2018, LncRNA PVT1 Triggers Cyto-Protective Autophagy and Promotes Pancreatic Ductal Adenocarcinoma Development Via the miR-20a-5p/ULK1 Axis. Mol Cancer, 17(1): 98.

[17] Cheng L, Han T, Zhang Z, et al., 2021, Identification and Validation of Six Autophagy-Related Long Non-Coding RNAs as Prognostic Signature in Colorectal Cancer. Int J Med Sci, 18(1): 88–98.

[18] Wang X, Dai C, Ye M, et al., 2021, Prognostic Value of an Autophagy-Related Long-Noncoding-RNA Signature for Endometrial Cancer. Aging (Albany NY), 13(4): 5104–5119.

[19] Pang K, Ran M-J, Zou F-W, et al., 2018, Long Non-Coding RNA LINC00857 Promotes Gastric Cancer Cell Proliferation and Predicts Poor Patient Survival. Oncol Lett, 16(2): 2119–2124.

[20] Li J, Xu Q, Wang W, et al., 2019, MIR100HG: A Credible Prognostic Biomarker and an Oncogenic LncRNA in Gastric Cancer. Biosci Rep, 39(4): BSR20190171.

[21] Zhang N, Zeng X, Sun C, et al., 2019, LncRNA LINC00963 Promotes Tumorigenesis and Radioresistance in Breast Cancer by Sponging miR-324-3p and Inducing ACK1 Expression. Mol Ther Nucleic Acids, 18: 871–881.

[22] Yu M, Yu S, Gong W, et al., 2019, Knockdown of Linc01023 Restrains Glioma Proliferation, Migration and Invasion by Regulating IGF-1R/AKT Pathway. J Cancer, 10(13): 2961–2968.

[23] Ren J, Zhang F-J, Wang J-H, et al., 2021, LINC01315 Promotes the Aggressive Phenotypes of

Papillary Thyroid Cancer Cells by Sponging miR-497-5p. Kaohsiung J Med Sci, 37(6): 459–467.

[24] Liang R, Zhang J, Zhang RM, et al., 2021, LINC01315 Silencing Inhibits the Aggressive Phenotypes of Colorectal Carcinoma by Sponging miR-205-3p. Biochem Biophys Res Commun, 534: 1033–1039.

[25] Sun W, Nie W, Wang Z, et al., 2020, Lnc HAGLR Promotes Colon Cancer Progression Through Sponging miR-185-5p and Activating CDK4 and CDK6 In Vitro and In Vivo. Onco Targets Ther, 13: 5913–5925.

[26] Suzuki HI, Kiyono K, Miyazono K, 2010, Regulation of Autophagy by Transforming Growth Factor-Beta (TGF-Beta) Signaling. Autophagy, 6(5): 645–647.

[27] Jin L, Luo C, Wu X, et al., 2021, LncRNA-HAGLR Motivates Triple Negative Breast Cancer Progression by Regulation of WNT2 Via Sponging miR-335-3p. Aging (Albany NY), 13(15): 19306–19316.